

## Direct Search for Dark Matter with DarkSide

*P Agnes*<sup>1</sup>, T Alexander<sup>2</sup>, A Alton<sup>3</sup>, K Arisaka<sup>4</sup>, H O Back<sup>5</sup>, B Baldin<sup>6</sup>, K Biery<sup>6</sup>, G Bonfini<sup>7</sup>, M Bossa<sup>8</sup>, A Brigatti<sup>9</sup>, J Brodsky<sup>5</sup>, F Budano<sup>10</sup>, L Cadonati<sup>2</sup>, F Calaprice<sup>5</sup>, N Canci<sup>5</sup>, A Candela<sup>7</sup>, H Cao<sup>5</sup>, M Cariello<sup>11</sup>, P Cavalcante<sup>7</sup>, A Chavarria<sup>12</sup>, A Chepurnov<sup>13</sup>, A G Cocco<sup>14</sup>, L Crippa<sup>9</sup>, D D'Angelo<sup>9</sup>, M D'Incecco<sup>7</sup>, S Davini<sup>15</sup>, M De Deo<sup>7</sup>, A Derbin<sup>16</sup>, A Devoto<sup>17</sup>, F Di Eusano<sup>5</sup>, G Di Pietro<sup>9</sup>, E Edkins<sup>18</sup>, A Empl<sup>15</sup>, A Fan<sup>14</sup>, G Fiorillo<sup>14</sup>, K Fomenko<sup>19</sup>, G Forster<sup>2</sup>, D Franco<sup>1</sup>, F Gabriele<sup>7</sup>, C Galbiati<sup>5</sup>, A Goretti<sup>5</sup>, L Grandi<sup>12</sup>, M Gromov<sup>13</sup>, M Y Guan<sup>20</sup>, Y Guardincerri<sup>6</sup>, B Hackett<sup>18</sup>, K Herner<sup>6</sup>, E V Hungerford<sup>15</sup>, Al Ianni<sup>7</sup>, An Ianni<sup>5</sup>, C Jollet<sup>21</sup>, K Keeter<sup>22</sup>, C Kendziora<sup>6</sup>, S Kidner<sup>23</sup>, V Kobychhev<sup>24</sup>, G Koh<sup>5</sup>, D Korablev<sup>19</sup>, G Korga<sup>15</sup>, A Kurlej<sup>2</sup>, P X Li<sup>20</sup>, B Loer<sup>5</sup>, P Lombardi<sup>9</sup>, C Love<sup>25</sup>, L Ludhova<sup>9</sup>, S Luitz<sup>25</sup>, Y Q Ma<sup>20</sup>, I Machulin<sup>27,28</sup>, A Mandarano<sup>10</sup>, S Mari<sup>10</sup>, J Maricic<sup>18</sup>, L Marini<sup>10</sup>, C J Martoff<sup>25</sup>, A Meregaglia<sup>21</sup>, E Meroni<sup>9</sup>, P D Meyers<sup>5</sup>, R Milincic<sup>18</sup>, D Montanari<sup>6</sup>, M Montuschi<sup>7</sup>, M E Monzani<sup>26</sup>, P Mosteiro<sup>5</sup>, B Mount<sup>22</sup>, V Muratova<sup>16</sup>, P Musico<sup>11</sup>, A Nelson<sup>5</sup>, S Odrowski<sup>7</sup>, M Okounkova<sup>5</sup>, M Orsini<sup>7</sup>, F Ortica<sup>29</sup>, L Pagani<sup>11</sup>, M Pallavicini<sup>11</sup>, E Pantic<sup>4,30</sup>, L Papp<sup>23</sup>, S Parmeggiano<sup>9</sup>, R Parsells<sup>5</sup>, K Pelczar<sup>31</sup>, N Pelliccia<sup>29</sup>, S Perasso<sup>1</sup>, A Pocar<sup>2</sup>, S Pordes<sup>6</sup>, D Pugachev<sup>27</sup>, H Qian<sup>5</sup>, K Randle<sup>2</sup>, G Ranucci<sup>9</sup>, A Razeto<sup>7</sup>, B Reinhold<sup>18</sup>, A Renshaw<sup>4</sup>, A Romani<sup>29</sup>, B Rossi<sup>5,14</sup>, N Rossi<sup>7</sup>, S D Rountree<sup>23</sup>, D Sablone<sup>15</sup>, P Saggese<sup>7</sup>, R Saldanha<sup>12</sup>, W Sands<sup>5</sup>, S Sangiorgio<sup>3,2</sup>, E Segreto<sup>7</sup>, D Semenov<sup>16</sup>, E Shields<sup>5</sup>, M Skorokhvatov<sup>27,28</sup>, O Smirnov<sup>19</sup>, A Sotnikov<sup>19</sup>, C Stanford<sup>5</sup>, Y Suvorov<sup>4</sup>, R Tartaglia<sup>7</sup>, J Tatarowicz<sup>25</sup>, G Testera<sup>11</sup>, A Tonazzo<sup>1</sup>, E Unzhakov<sup>16</sup>, R B Vogelaar<sup>23</sup>, M Wada<sup>5</sup>, S Walker<sup>14</sup>, H Wang<sup>4</sup>, Y Wang<sup>20</sup>, A Watson<sup>25</sup>, S Westerdale<sup>5</sup>, M Wojcik<sup>31</sup>, A Wright<sup>5</sup>, X Xiang<sup>5</sup>, J Xu<sup>5</sup>, C G Yang<sup>20</sup>, J Yoo<sup>6</sup>, S Zavatarelli<sup>11</sup>, A Zec<sup>2</sup>, C Zhu<sup>5</sup>, and G Zuzel<sup>31</sup>

<sup>1</sup> APC, Université Paris Diderot, Sorbonne Paris Cité, Paris 75205, France

<sup>2</sup> Amherst Center for Fundamental Interactions and Physics Department, University of Massachusetts, Amherst, MA 01003, USA

<sup>3</sup> Physics and Astronomy Department, Augustana College, Sioux Falls, SD 57197, USA

<sup>4</sup> Physics and Astronomy Department, University of California, Los Angeles, CA 90095, USA

<sup>5</sup> Department of Physics, Princeton University, Princeton, NJ 08544, USA

<sup>6</sup> Fermi National Accelerator Laboratory, Batavia, IL 60510, USA

<sup>7</sup> Laboratori Nazionali del Gran Sasso, Assergi (AQ) 67010, Italy

<sup>8</sup> Gran Sasso Science Institute, L'Aquila 67100, Italy

<sup>9</sup> Physics Department, Università degli Studi and INFN, Milano 20133, Italy

<sup>10</sup> Physics Department, Università degli Studi Roma Tre and INFN, Roma 00146, Italy

<sup>11</sup> Physics Department, Università degli Studi and INFN, Genova 16146, Italy



<sup>12</sup> Kavli Institute, Enrico Fermi Institute and Dept. of Physics, University of Chicago, Chicago, IL 60637, USA

<sup>13</sup> Skobeltsyn Institute of Nuclear Physics, Lomonosov Moscow State University, Moscow 119991, Russia

<sup>14</sup> Physics Department, Università degli Studi Federico II and INFN, Napoli 80126, Italy

<sup>15</sup> Department of Physics, University of Houston, Houston, TX 77204, USA

<sup>16</sup> St. Petersburg Nuclear Physics Institute, Gatchina 188350, Russia

<sup>17</sup> Physics Department, Università degli Studi and INFN, Cagliari 09042, Italy

<sup>18</sup> Department of Physics and Astronomy, University of Hawai'i, Honolulu, HI 96822, USA

<sup>19</sup> Joint Institute for Nuclear Research, Dubna 141980, Russia

<sup>20</sup> Institute of High Energy Physics, Beijing 100049, China

<sup>21</sup> IPHC, Université de Strasbourg, CNRS/IN2P3, Strasbourg 67037, France

<sup>22</sup> School of Natural Sciences, Black Hills State University, Spearfish, SD 57799, USA

<sup>23</sup> Physics Department, Virginia Tech, Blacksburg, VA 24061, USA

<sup>24</sup> Institute for Nuclear Research, National Academy of Sciences of Ukraine, Kiev 03680, Ukraine

<sup>25</sup> Physics Department, Temple University, Philadelphia, PA 19122, USA

<sup>26</sup> SLAC National Accelerator Laboratory, Menlo Park, CA 94025, USA

<sup>27</sup> National Research Centre Kurchatov Institute, Moscow 123182, Russia

<sup>28</sup> National Research Nuclear University MEPhI (Moscow Engineering Physics Institute), 115409 Moscow, Russia

<sup>29</sup> Chemistry, Biology and Biotechnology Department, Università degli Studi and INFN, Perugia 06123, Italy

<sup>30</sup> Physics Department, University of California, Davis, CA 95616, USA

<sup>31</sup> Smoluchowski Institute of Physics, Jagiellonian University, Krakow 30059, Poland

<sup>32</sup> Lawrence Livermore National Laboratory, 7000 East Avenue, Livermore, CA 94550

E-mail: [pagnes@in2p3.fr](mailto:pagnes@in2p3.fr)

**Abstract.** The DarkSide experiment is designed for the direct detection of Dark Matter with a double phase liquid Argon TPC operating underground at *Laboratori Nazionali del Gran Sasso*. The TPC is placed inside a 30 tons liquid organic scintillator sphere, acting as a neutron veto, which is in turn installed inside a 1 kt water Cherenkov detector. The current detector is running since November 2013 with a 50 kg atmospheric Argon fill and we report here the first null results of a Dark Matter search for a  $(1422 \pm 67)$  kg.d exposure. This result correspond to a 90% CL upper limit on the WIMP-nucleon cross section of  $6.1 \times 10^{-44}$  cm<sup>2</sup> (for a WIMP mass of 100 GeV/c<sup>2</sup>) and it's currently the most sensitive limit obtained with an Argon target.

## 1. Introduction

Our knowledge of the energy balance of the Universe is derived only by indirect observations. We know that the baryonic matter (the so called luminous matter) only accounts for roughly the 5% of the energy content, while Dark Energy and Dark Matter are estimated to provide the larger contributions, which account for the 68% and the 27% respectively (according to the recent results of the Planck experiment).

The first hypotheses on the existence of Dark Matter date back to the beginning of the 20th century and they are presently well supported by several indirect observations. In spite of this, the knowledge of the nature of these particles, not predicted by the Standard Model, is extremely poor. One of the most favored candidate is known as WIMP, an acronym for Weakly Interactive Massive Particle. These particles are supposed to have masses in the GeV-TeV range, to not interact strongly nor electromagnetically, but only through gravitational and weak forces. The current upper limit on the WIMP-nucleon cross section, extremely low, is  $7.6 \times 10^{-46}$  cm<sup>2</sup> for 33 GeV WIMP mass at 90% CL [1].

The indirect search for WIMPs can be performed by looking for ordinary decay products of WIMP-WIMP annihilation in the Universe or by producing WIMPs in collider experiments;

the direct detection channel can be exploited by searching for nuclear recoils induced by elastic scattering of WIMPs on ordinary nuclei.

A detector for the direct detection must satisfy some requirements: a large active mass; low energy thresholds, since a typical nuclear recoil only deposits less than 100 keV; strong background suppression. Such a detector can be designed to collect the ionization charges, the scintillation light or the phonons produced inside the sensitive medium by the recoiling nucleus. Several experiments are currently running around the world, exploiting different targets and detection techniques, and many among them are designed to access to more than one of those quantities at the same time.

## 2. Direct Detection of Dark Matter in Noble Liquids

Noble liquids are suitable for direct detection of Dark Matter: they are dense, inexpensive and easy to be purified (a detector can be scaled up to large volumes) and they have high ionization and scintillation yields (roughly one electrons every 20 eV and 40k photons/MeV respectively).

When a charged particle interacts within noble liquids, it loses energy by both ionization and excitation, according to the stopping power of the interacting particle. The excited atoms de-excite producing a prompt light signal in the UV range (scintillation light, called S1 in the following). Electrons and ions produced by ionization can be separated by means of an electric field. A fraction of free electrons, however, undergo to the recombination process with ions produced along the particle track. The recombined atom is in an excited state and the de-excitation increases the S1 signal. The recombination effect is larger at higher ionization densities, and hence stronger for nuclear recoils with respect to electronic recoils. As a result, nuclear and electronic recoils can be discriminated with a rejection factor of the order of  $10^2$ - $10^3$  [2, 3].

Liquid noble gases experiments, thanks to the double phase TPC technique, are suitable for measuring both the scintillation and the ionization components: the ionization electrons are drifted up to a gaseous layer, lying on the top of the liquid noble volume, and extracted by means of an applied electric field. During the extraction, a second light emission occurs (called S2), thanks to the electro-luminescence effect, proportional to the number of ionization electrons.

The main two noble liquid targets used in currently running experiments are Argon and Xenon. The predicted interaction cross section is slightly different, being larger at low WIMP masses for Xenon. Xenon is denser and highly radio-purer with respect to Argon. Further, the Xenon technology is more advanced and already provided the most stringent limits on the WIMP-nucleon cross section.

The delay of the Argon technology with respect to the Xenon based one is due to the non negligible content of  $^{39}\text{Ar}$  in atmospheric Argon.  $^{39}\text{Ar}$  is a  $\beta$  emitter, with a Q-value of 565 keV and half life of about 269 years. The typical activity of atmospheric Argon, due to cosmic rays activation, is of the order of 1 Bq/kg and this always prevented the built of a large detector for rare events experiments. The problem can be solved thanks to the recent development of the underground Argon (UAr) extraction technique. This Argon is depleted in  $^{39}\text{Ar}$  and a depletion fraction larger than 150 has been achieved, as shown in Figure 1. A mass production of underground Argon seems also to be possible at affordable price for future large scale detectors.

Liquid Argon has the advantage of an extremely high discrimination power thanks to the Pulse Shape Discrimination (PSD). The excited Argon atom has two states, with two different decay time constant (the single state, with  $\tau_1 \sim 7$  ns and the triplet state with  $\tau_2 \sim 1600$  ns). While a nuclear recoil mostly excites the fast state, a typical electronic recoil mostly excites the slow one. Thus, simply looking at the fraction of S1 light that occurs in the first tens of nanoseconds of the signal itself, it is possible to discriminate between nuclear and electronic recoils up to a factor  $10^8$  [5]. In Liquid Xenon the two time constants are similar ( $\tau_1 \sim 22$  ns and  $\tau_2 \sim 45$  ns) and the implementation of this technique is prevented [6].

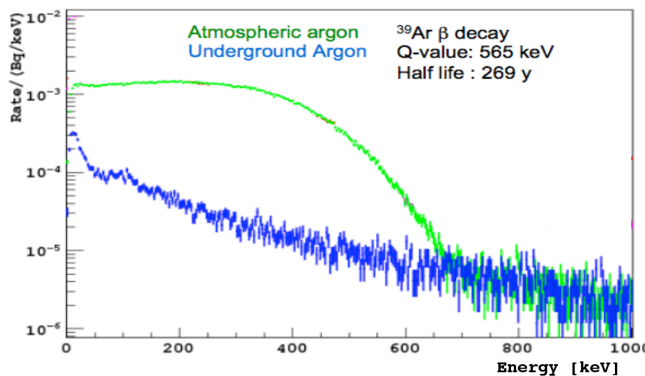


**Figure 1.** Comparison between the atmospheric Argon (green) and the underground Argon (blue) spectra, as measured at the KURF underground laboratory. The depletion factor results to be  $> 150$  [4].

### 3. The DarkSide experiment

#### 3.1. The DarkSide program

The DarkSide goal is a background free experiment with a multi-ton scale double phase liquid Argon TPC. In order to accomplish such an ambitious result, the DarkSide collaboration is proceeding through a staged approach. The first prototype (Darkside-10), built in Princeton and running until 2013, proved the stability of the detector and a light yield of about 9 photoelectrons/keV was measured. In the current configuration (Darkside-50) the active mass of the detector has been increased from 10 kg to 50 kg. The full experimental setup includes also a spherical liquid scintillator detector acting as neutron veto and surrounding the TPC, and a water Cherenkov detector for vetoing muons, hosting the sphere.

In spite of the current atmospheric Argon fill and the calibration purposes, the DarkSide-50 first physics results are remarkable and will be discussed in the following.

It is currently under discussion the design of the future phase detector, with a more competitive physics potential. The veto sphere presently installed is already designed in order to host a larger cryostat, so the active mass can easily be scaled up to few tons. The commissioning of the future detector is foreseen to start after the end of the current phase (expected in 2017).

#### 3.2. The DarkSide detector

The detector is installed underground, at *Laboratori Nazionali del Gran Sasso* (LNGS, in Italy), under 3400 m.w.e of rock working as a shield from cosmic rays and it has been realized with highly radiopure materials.

The core of the DarkSide experiment is the double phase liquid Argon time projection chamber, 36 cm diameter  $\times$  36 cm height, and filled with roughly 46.7 kg of Liquid Argon (LAr). Two arrays of 19 photo-multipliers are pointing to the center of the volume from the top and from the bottom surfaces (two quartz windows). On the top of the liquid, a 1 cm height gas region is created by heating the LAr. A uniform electric field (200 V/cm) is maintained along the vertical axis of the cylinder and a stronger electric field is present in the gas region (2800 V/cm) for the extraction of ionization electrons.

All the internal surfaces of the TPC are reflective and coated with TPB (TetraPhenylButadiene), a wavelength-shifter required in order to convert the 128 nm LAr scintillation light in visible one, to match the photocathode sensitivity.

The cryostat is placed inside a 4 m diameter sphere, filled with an organic Liquid Scintillator and equipped with 110 PMTs (8 inches), acting as a neutron veto. The solution is made by 50% Pseudocumene (PC) and TriMethylButadiene (TMB), the latter being a molecule, loaded with Boron, with a very high neutron capture cross section. Also PPO in 5 g/l concentration is added

to reduce the light quenching. The mean lifetime of neutrons inside this solution is of the order of  $2 \mu\text{s}$  and the veto efficiency has been estimated to be higher than 99.9%. The main goal of the neutron veto is the rejection of WIMP-like interactions (nuclear recoils) produced inside the TPC by radiogenic and cosmogenic neutrons; moreover is designed to work actively, not only shielding the TPC from the environment, but also measuring the real neutron background.

The Neutron Veto sphere is then placed inside a 10 kton water tank, with 80 PMTs (8 inches) installed on the side and on the bottom, acting as a Cherenkov detector for the surviving cosmic muons at the depth of the Laboratories. A sketch of the three nested detectors is shown in Figure 2.

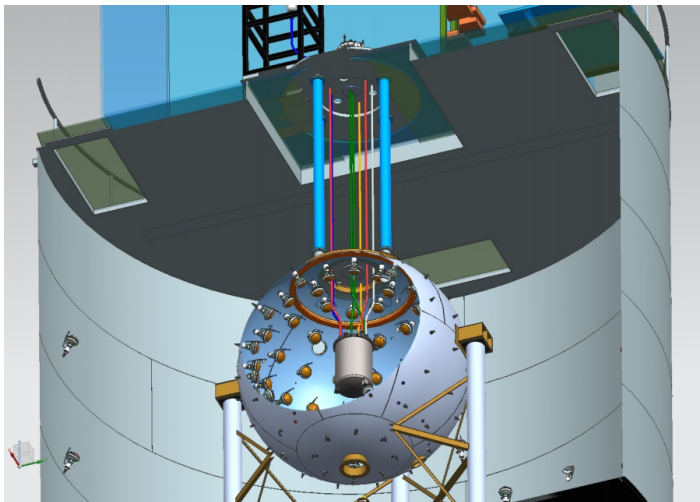


**Figure 2.** The nested detector system of DarkSide-50. The outermost gray cylinder is the Water Cherenkov Detector, the sphere is the Liquid Scintillator Veto, and the gray cylinder at the center of the sphere is the LAR TPC cryostat.

## 4. The First Results

### 4.1. Detector calibration and stability

The calibration of the detector has been realized with the insertion of  $^{83}\text{Kr}$  inside the Argon circulation loop, a common practice for noble liquids experiment. This radio-nuclide emits two low energy gammas (for a total deposit of 41.5 keV) and has a mean life of 1.8 hours. The position of the 41.5 keV peak over the  $^{39}\text{Ar}$   $\beta$ -spectrum allows to measure the light yield of the detector:  $7.9 \pm 0.4$  photo-electrons/keV without the electric field and  $\sim 7.0$  photo-electrons/keV at 200 V/cm.

The stability of the detector response can also be evaluated selecting the events populating the 41.5 keV peak. While the maximum electron drift time, for the 200 V/cm electric field, is set to  $375 \mu\text{s}$  ( $v_{\text{drift}} \sim 0.93 \text{ mm}/\mu\text{s}$ ), the measured electron lifetime is larger than 5 ms. The internal non-uniformity both in terms of light and electrons collection have been evaluated as well.

For the neutron expectation band, it is safe to adopt the results of the SCENE experiment [8], a calibration experiment designed to study the nuclear recoils in LAr with a neutron beam and a small TPC. The reduced dimensions of the TPC are convenient in order to obtain a clean sample of single scattering events and nuclear recoils have been studied for different neutron energies and electric fields.

A calibration campaign with neutron ( $\text{AmBe}$ ) and gamma ( $^{57}\text{Co}$ ,  $^{133}\text{Ba}$  and  $^{137}\text{Cs}$ ) sources at different energies is currently ongoing.

#### 4.2. Background rejection

A WIMP interacting inside the sensitive volume is expected to hit a nucleus and to produce a nuclear recoil. As already mentioned, the main tool for rejecting electron recoils that trigger the TPC is the the Pulse Shape Discrimination (up to a factor  $10^8$ ). Exploiting the S2/S1 ratio will increase the rejection power by an additional factor  $10^2 \div 10^3$ .

The most dangerous source of WIMP-like background is represented by cosmogenic and radiogenic neutrons. Some of these events, those with multiple interaction inside the TPC, can be rejected since they produce a multiple ionization signal. The neutrons interacting only once in the TPC are likely to be captured inside the  $4\pi$  liquid scintillator surrounding veto. A capture on  $^{10}\text{B}$  results in the production of  $^7\text{Li}$  and  $\alpha$  particle. The  $\alpha$  energy is 1.47 MeV, quenched to  $\sim 50$  keV. With a branching ratio of 94%, a 480 keV  $\gamma$  is also emitted. The measured light yield in the veto scintillator ( $\sim 0.52$  pe/keV) is large enough to detect the  $\alpha$  also when no  $\gamma$  is emitted.

The number of cosmogenic neutrons that penetrate the veto undetected is negligible in a multi-year DarkSide-50 exposure (from calculation). Concerning the internal radioactivity, the major source of neutrons are the PMTs (to be replaced in a future detector by cleaner ones) and the total expected yield is about 100 n/y. From Geant4 based simulation, only  $5 \times 10^{-4}$  of them are expected to interact once in the TPC and to escape the veto without leaving any detectable signal ( $< 30$  pe). This fraction can vary by 20%, because of the large uncertainty on the quenching factor of the  $\alpha$ 's.

Finally, a fiducialization is applied to the active volume, in order to prevent contamination from  $\alpha$  surface emissions (from raw materials qualification, they are expected to be  $< 10/\text{m}^2/\text{day}$ ), removing events that are originated within 2 cm from the walls. After this cut, the fiducial volume is reduced to 36.9 kg of LAr.

#### 4.3. Extrapolation of the limit

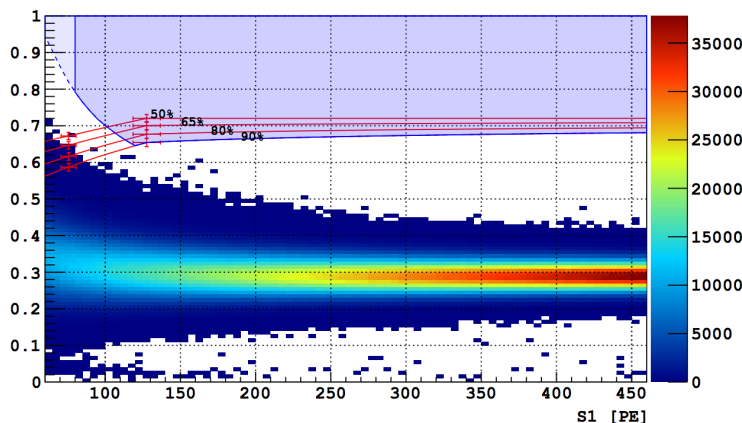


**Figure 3.** Distribution of the events in the scatter plot of S1 vs. f90 after all quality and physics cuts. Shaded blue with solid blue outline: Dark Matter search box in the f90 vs. S1 plane. Percentages label the f90 acceptance contours for nuclear recoils drawn connecting points (shown with error bars) determined from the corresponding SCENE measurements.

The first result, corresponding to a total lifetime of 47.2 days, is shown in Figure 3 [7]. The plot vertical axis corresponds to the PSD parameter (f90 or the fraction of S1 signal that occurs in the first 90 ns of the signal itself). The f90 parameter is known to be  $\sim 0.3$  for electronic recoils and  $\sim 0.7$  for nuclear recoils. The selected energy window for nuclear recoils extends from roughly 40 to 200 keV<sub>nr</sub>, namely 8 to 40 keV<sub>ee</sub> (electron recoil equivalent).

The Dark Matter search box shown in the plot is obtained by intersecting the 90% nuclear recoil acceptance line from the SCENE experiment with the curve corresponding to a leakage of  $^{39}\text{Ar}$  events of 0.01 events/(5-pe bin). The leakage curves are obtained by fitting the f90 distributions for any fixed energy according to the Hinkley model [10].

There are no events in the upper part of the plot, but a large number of electronic recoils (mainly due to the  $^{39}\text{Ar}$ ) populate the lower region. This result has been obtained with atmospheric Argon runs and the collected statistics corresponds to roughly 20 years of DS-50 run with Depleted Argon.

A first limit on the WIMP-nucleon cross section can be derived from these data, even if a physics result was not the main goal of this calibration campaign. The limit, compared in Figure 4 with the current best results from LUX (a LXe detector) and other experiments, correspond to  $6.1 \times 10^{-44} \text{ cm}^2$  (90% CL) for 100 GeV WIMP mass and it is currently the most stringent one obtained with a Liquid Argon target.

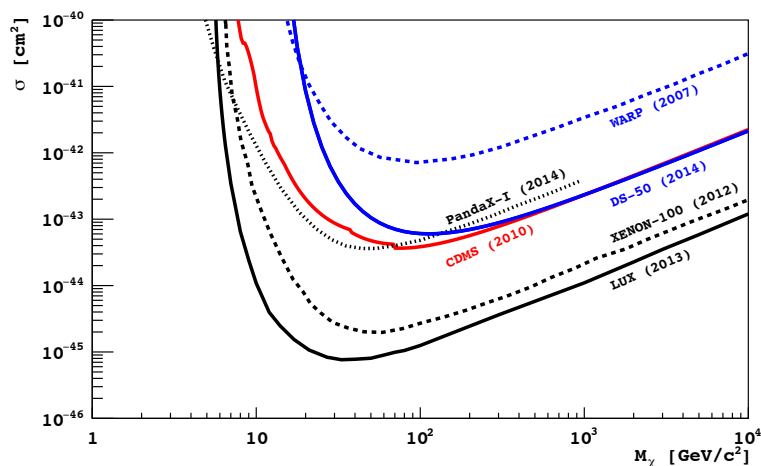


**Figure 4.** Spin-independent WIMP-nucleon cross section 90% C.L. exclusion plot for the DarkSide-50 atmospheric Argon campaign (Solid Blue Curve) compared with results from LUX [1] (Solid Black Curve) and other experiments.

## 5. Conclusions and outlook

The DarkSide-50 detector is successfully running and taking data since November 2013. The calibration campaign is almost concluded and the data available so far (corresponding to 50 days lifetime) provided a first physics result.

This result confirms the effectiveness of the Pulse Shape Discrimination: the present exposure of  $(1422 \pm 67) \text{ kg}\cdot\text{d}$  with atmospheric Argon, corresponding to 215000 kg.d of running with underground Argon, proves that DarkSide-50 could run for two decades with underground Argon and be free of  $^{39}\text{Ar}$  background. In the meanwhile, a first batch of 150 kg of UAr has been shipped to LNGS and the insertion of the liquid inside the cryostat is expected at the end of February 2015.

The design of the next phase detector is currently under discussion. The expected sensitivity for the WIMP-nucleon cross section will be of the order of  $10^{-47} \text{ cm}^2$  in a few years exposure, thanks to a ton-scale active mass of underground Argon.

## References

- [1] D. S. Akerib et al. (LUX Collaboration), Phys. Rev. Lett. 112, 091303 (2014).
- [2] Benetti et al. (ICARUS) 1993.
- [3] The WARP Collaboration, arXiv:0701286.
- [4] arXiv:1204.6011
- [5] WARP Astr. Phys 28, 495 (2008)
- [6] arXiv.org:1106.2209
- [7] The DarkSide Collaboration, arXiv:1410.0653.
- [8] T. Alexander et al. (SCENE Collaboration), Phys. Rev. D 88, 092006 (2013).
- [9] P. Cushman et al. (APS Community Summer Study 2013), arXiv:1310.8327.
- [10] The DEAP Collaboration, arXiv:0801.1531v4.